



## OPEN Dual FDG/PSMA PET imaging to predict lesion-based progression of mCRPC during PSMA-RLT

Florian Rosar<sup>1</sup>, Caroline Burgard<sup>1</sup>, Scott David<sup>1</sup>, Robert J. Marlowe<sup>2</sup>, Mark Bartholomä<sup>1</sup>, Stephan Maus<sup>1</sup>, Sven Petto<sup>1</sup>, Fadi Khreish<sup>1</sup>, Andrea Schaefer-Schuler<sup>1</sup> & Samer Ezziddin<sup>1</sup>✉

Candidates for prostate-specific membrane antigen (PSMA)-targeted radioligand therapy (RLT) of metastatic castration-resistant prostate cancer (mCRPC) frequently have “mismatch” lesions with pronounced 18-fluorodeoxyglucose (<sup>18</sup>F)FDG but attenuated PSMA ligand uptake on positron emission tomography (PET). However, no quantitative criteria yet exist to identify mismatch lesions and predict their response to RLT. To define such criteria, we retrospectively analyzed 267 randomly selected glucometabolic mCRPC metastases from 22 patients. On baseline PET, we determined [<sup>18</sup>F]FDG and [<sup>68</sup>Ga]Ga-PSMA-11 maximum standardized uptake value (SUV<sub>max</sub>), and calculated the [<sup>18</sup>F]FDG SUV<sub>max</sub>/[<sup>68</sup>Ga]Ga-PSMA-11 SUV<sub>max</sub> quotient (FPQ). From follow-up [<sup>18</sup>F]FDG PET after two lutetium-177-PSMA-617 RLT cycles, we evaluated the treatment response and categorized the lesions into three subgroups (partial remission, stable disease, progression) based on change in [<sup>18</sup>F]FDG SUV<sub>max</sub>. Lastly, we compared the baseline PET variables in progressing versus non-progressing lesions. Variables differing significantly, and a score incorporating them, were assessed via receiver operator characteristic (ROC) curve analysis, regarding ability to predict lesional progression, with area under the curve (AUC) as metric. Cut-offs with optimal sensitivity and specificity were determined using the maximum value of Youden’s index. Fifty-one of 267 lesions (19.1%) progressed, 102/267 (38.2%) manifested stable disease, and 114/267 (42.7%) partially responded after two RLT cycles. At baseline, median [<sup>68</sup>Ga]Ga-PSMA-11 SUV<sub>max</sub> was significantly lower ( $p < 0.001$ ), median FPQ significantly higher ( $p < 0.001$ ), and median [<sup>18</sup>F]FDG SUV<sub>max</sub> similar in progressing versus non-progressing lesions. [<sup>68</sup>Ga]Ga-PSMA-11 SUV<sub>max</sub> and FPQ showed predictive power regarding progression (AUCs: 0.89, 0.90). An introduced clinical score combining both further improved predictive performance (AUC: 0.94). Optimal cut-offs to foretell progression were: [<sup>68</sup>Ga]Ga-PSMA-11 SUV<sub>max</sub> < 11.09 (88.2% sensitivity, 81.9% specificity), FPQ ≥ 0.92 (90.2% sensitivity, 78.7% specificity), clinical score ≥ 6/9 points (88.2% sensitivity, 87.5% specificity). At baseline, a low [<sup>68</sup>Ga]Ga-PSMA-11 SUV<sub>max</sub> and a high FPQ predict early lesional progression under RLT; [<sup>18</sup>F]FDG SUV<sub>max</sub> does not. A score combining [<sup>68</sup>Ga]Ga-PSMA-11 SUV<sub>max</sub> and FPQ predicts early lesional progression even more effectively and might therefore be useful to quantitatively identify mismatch lesions.

**Keywords** mCRPC, PSMA, FDG, Mismatch, Radioligand therapy

### Abbreviations

<sup>18</sup> F	Fluorine-18
<sup>68</sup> Ga	Gallium-68
<sup>177</sup> Lu	Lutetium-177
ADT	Androgen deprivation therapy
AUC	Area under the receiver operator characteristic curve
CT	Computed tomography
DIPP	Dual imaging progression prediction
ECOG	Eastern cooperative oncology group
FDG	Fluorodeoxyglucose
NAAD	Novel androgen axis drugs
PERCIST	Positron emission tomography response criteria in solid tumors

<sup>1</sup>Departments of Nuclear Medicine, Saarland University – Medical Center, Kirrberger Str. 100, Geb. 50, 66421 Homburg, Germany. <sup>2</sup>Spencer-Fontayne Corporation, Jersey City, NJ, USA. ✉email: samer.ezziddin@uks.eu

PET	Positron emission tomography
p.i.	Post-injection
PSA	Prostate-specific antigen
PSMA	Prostate-specific membrane antigen
RLT	Radioligand therapy
ROC	Receiver operator characteristic
SD	Standard deviation
SUV <sub>max</sub>	Maximum standardized uptake value

Radioligand therapy (RLT) targeted at prostate-specific membrane antigen (PSMA) has emerged, and gained regulatory approval, as a promising new option for palliation and/or increased survival for many patients with metastatic castration-resistant prostate cancer (mCRPC)<sup>1–3</sup>. Also a target for positron emission tomography (PET) imaging of prostate cancer<sup>4–12</sup>, PSMA is a transmembrane glycoprotein that is typically, but not invariably, overexpressed on mCRPC cells<sup>13–15</sup>. Ample tumoral expression of this target, established on PET, is, unsurprisingly, the major eligibility requirement for PSMA-directed RLT of mCRPC<sup>1–3,16</sup>.

Prostate cancer cells with an aggressive phenotype, especially mCRPC cells, also frequently abundantly express glucose transporter 1 (GLUT1) due to heightened dependence on glucose intake and aerobic glycolysis for energy as mutations and tumor burden increase<sup>17,18</sup>. As on many other malignant cell types, GLUT1 overexpression on prostate cancer cells is reflected by uptake of the fluorine-18-conjugated glucose analogue fluorodeoxyglucose (<sup>18</sup>F]FDG), shown on PET<sup>19</sup>. Higher <sup>18</sup>F]FDG uptake now is well-recognized to correlate with prognostically-unfavorable pathological factors in prostate cancer in general<sup>20,21</sup>, and with poor outcomes in men receiving systemic treatment of mCRPC, including PSMA-targeted RLT<sup>18,22–25</sup>. As a result, <sup>18</sup>F]FDG PET/computed tomography (CT) increasingly is being applied in mCRPC, to provide prognostic and/or predictive data<sup>3,16,26–29</sup>.

mCRPC lesions with high GLUT1 expression but attenuated or absent PSMA expression, as evidenced by uptake of the respectively-targeted radiotracers on PET, are termed “mismatch” lesions<sup>30</sup>. Due to the perceived reduced efficacy of RLT in mismatch lesions, the presence of such findings, indeed, sometimes even of a single mismatch lesion<sup>31</sup>, has been used as an exclusion criterion for PSMA-targeted RLT<sup>32–34</sup>. However, no quantitative uptake-related criteria based on both <sup>18</sup>F]FDG PET and PSMA-targeted PET exist yet to identify such lesions and to predict their response to RLT. We therefore performed a retrospective analysis of mCRPC metastases seeking to use quantitative PET variables to identify PSMA ligand/<sup>18</sup>F]FDG uptake profiles that predict RLT-refractory/resistant mCRPC lesions. Such characterization of mismatch lesions potentially will aid treatment-related decision-making in candidates for PSMA-targeted RLT.

## Materials and methods

### Endpoints

The first endpoint was each lesion's uptake of [<sup>68</sup>Ga]Ga-PSMA-11 and of [<sup>18</sup>F]FDG, reflected by the maximum standardized uptake value (SUV<sub>max</sub>) of each radiotracer, on PET scans acquired before [<sup>177</sup>Lu]Lu-PSMA-617 RLT, i.e. at baseline. As part of this endpoint, we also calculated the pre-RLT [<sup>18</sup>F]FDG SUV<sub>max</sub>/[<sup>68</sup>Ga]Ga-PSMA-11 SUV<sub>max</sub> quotient (FPQ) for each individual lesion.

The second endpoint was the evaluation of each lesion's response to two RLT cycles, based on changes in the [<sup>18</sup>F]FDG SUV<sub>max</sub> between the baseline [<sup>18</sup>F]FDG PET/CT scan and a follow-up [<sup>18</sup>F]FDG scan acquired after the second cycle.

The third endpoint was the comparison of baseline [<sup>68</sup>Ga]Ga-PSMA-11 SUV<sub>max</sub>, baseline [<sup>18</sup>F]FDG SUV<sub>max</sub>, and baseline FPQ in the subgroup of progressing lesions versus the subgroup of lesions with disease stability or partial response after the two RLT administrations, and determination of adequate cut-off values of these variables to predict lesional outcome.

The last endpoint, based on these comparisons, was the development and preliminary assessment of a score to use baseline quantitative PET variables to predict whether a lesion would progress early in the course of RLT.

### Lesions, patients, and ethics

The analysis included a sample of [<sup>18</sup>F]FDG-positive lesions in consecutive eligible patients with mCRPC who received two cycles of [<sup>177</sup>Lu]Lu-PSMA-617 RLT. Eligible patients had to have available PET imaging data from three scans: (1) baseline (pre-RLT) [<sup>68</sup>Ga]Ga-PSMA-11 PET/CT, (2) baseline [<sup>18</sup>F]FDG PET/CT, and (3) follow-up [<sup>18</sup>F]FDG PET/CT acquired shortly after completion of the two RLT cycles (Fig. 1). All patients received [<sup>177</sup>Lu]Lu-PSMA-617 RLT within a prospective patient registry (REALITY Study, NCT04833517). The analyzed imaging and treatment took place at the Saarland University Medical Center between 21 January 2019 and 21 December 2022. The selection of [<sup>18</sup>F]FDG-positive target lesions was random and did not consider uptake in PSMA ligand PET/CT.

A total of 267 lesions from 22 men (up to 14 per patient) were included in this analysis. Table 1 shows characteristics of the lesions and of the study sample. The analyzed lesions were mostly (almost 80%) in the skeleton. The patients tended to have late-stage or end-stage disease and were heavily pretreated. They received the PSMA-targeted RLT on a compassionate use basis according to §13 (2b) of the German Pharmaceutical Act. Patients gave written informed consent, which also covered participation in the registry and permission for de-identified patient data to be published in scientific communications. The study was approved by the local institutional review board (ethics committee approval number 140/17, 13 July 2017).

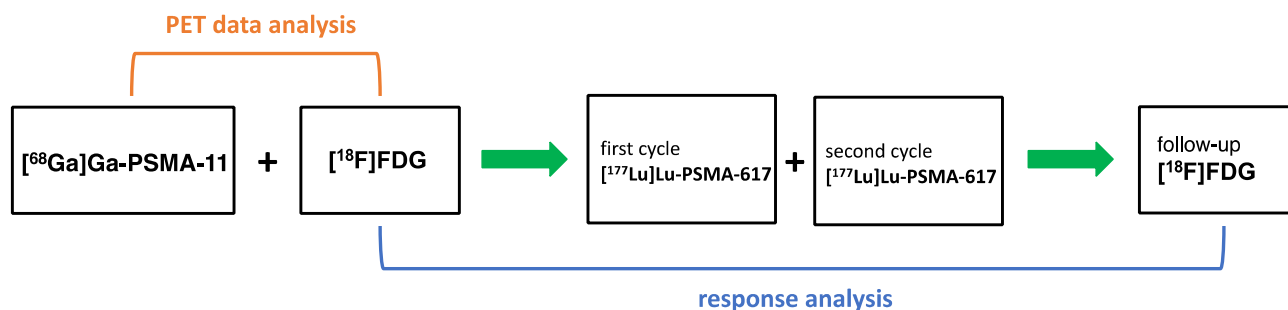


**Figure 1.** Schematic summary of study design.

Characteristic	Value
Age [yr]	71 (55–84)
PSA at baseline [ng/mL], median (minimum–maximum)	469 (0.08–2907)
ECOG performance status category at baseline, % (n)	
0	14% (3)
1	45% (10)
≥ 2	41% (9)
Prior treatment, % [no.]	
Prostatectomy	55% (12)
Radiation therapy	64% (14)
ADT	100% (22)
NAAD	100% (22)
Chemotherapy	
Any	77% (17)
Docetaxel	77% (17)
Cabazitaxel	45% (10)
Other	14% (3)
Radium-223	14% (3)
$[^{177}\text{Lu}]\text{Lu-PSMA-617}$ RLT activities [GBq], median (minimum–maximum)	
First activity	8.6 (1.1–10.6)
Second activity	8.2 (1.5–9.3)
Cumulative activity	16.7 (2.6–19.4)
Target lesions category, n (%)	
Any	267 (100%)
Lymph node	49 (18.4%)
Bone	212 (79.4%)
Liver	6 (2.2%)
Number per patient	
Mean ± SD	12 ± 4
Median (minimum–maximum)	14 (1–14)

**Table 1.** Characteristics of the patients cohort and target lesions. ADT androgen deprivation therapy, ECOG eastern cooperative oncology group, NAAD novel androgen access drugs, PSA, prostate-specific antigen.

### PET/CT

Initial  $[^{68}\text{Ga}]\text{Ga-PSMA-11}$  PET/CT and  $[^{18}\text{F}]\text{FDG}$  PET/CT were performed a mean ± standard deviation (SD)  $25 \pm 23$  d and  $18 \pm 22$  d, respectively, before PSMA-RLT started. The mean time between baseline  $[^{68}\text{Ga}]\text{Ga-PSMA-11}$  and baseline  $[^{18}\text{F}]\text{FDG}$  PET/CT was  $6 \pm 8$  d. The follow-up  $[^{18}\text{F}]\text{FDG}$  PET/CT, acquired after two cycles PSMA-RLT, took place  $122 \pm 65$  d after the baseline  $[^{18}\text{F}]\text{FDG}$  PET/CT scan. Both  $[^{68}\text{Ga}]\text{Ga-PSMA-11}$  PET/CT and  $[^{18}\text{F}]\text{FDG}$  PET/CT were performed ~ 60 min after intravenous injection of the radiotracer and a subsequent 500-mL infusion of NaCl 0.9%. A mean ± SD  $142 \pm 23$  MBq of  $[^{68}\text{Ga}]\text{Ga-PSMA-11}$ ,  $246 \pm 42$  MBq of  $[^{18}\text{F}]\text{FDG}$  (baseline scan), and  $259 \pm 35$  MBq of  $[^{18}\text{F}]\text{FDG}$  (follow-up scan) were given. Patients fasted at least 4 h before each  $[^{18}\text{F}]\text{FDG}$  infusion, and were instructed to void shortly before all PET/CT scans. Imaging was carried out applying standard protocols<sup>35,36</sup>. Whole-body PET images were acquired from vertex to mid-femur, using 3 min ( $[^{68}\text{Ga}]\text{Ga-PSMA-11}$ ) or 2 min ( $[^{18}\text{F}]\text{FDG}$ ) per bed position, with a 21.4-cm extended field-of-view. A Biograph 40 mCT scanner (Siemens Medical Solutions, Knoxville, TN, USA) was employed. For attenuation

correction and anatomical localization, low-dose CT was performed together with the PET, using a 120-keV X-ray tube voltage. The tube current was modulated with CARE Dose4D software (Siemens Healthineers, Erlangen, Germany), with 30 mAs as the reference. PET datasets were reconstructed with an iterative 3-dimensional ordered-subset expectation maximization algorithm (3 iterations, 24 subsets) with gaussian filtering (5 mm full width at half maximum) and a 3 mm slice thickness. Besides attenuation correction, random, decay, and scatter correction were done.

### PET/CT data analysis

Firstly, [<sup>18</sup>F]FDG-positive target lesions of mCRPC were randomly selected and analyzed at baseline [<sup>18</sup>F]FDG PET/CT. Subsequently, the same target lesions were analyzed on the baseline [<sup>68</sup>Ga]Ga-PSMA-11 PET/CT scan. Care was taken to exclude foci representing characteristic inflammatory changes on [<sup>18</sup>F]FDG PET/CT, e.g. pulmonary inflammatory changes or reactive-inflammatory lymph nodes. For each target lesion and both radiotracer SUV<sub>max</sub> was quantified, applying Syngo.via (Siemens Healthineers, Erlangen, Germany). In addition, FPQ was calculated for each individual lesion by dividing SUV<sub>max</sub> of [<sup>18</sup>F]FDG by SUV<sub>max</sub> of [<sup>68</sup>Ga]Ga-PSMA-11.

### RLT response classification

For each target lesion selected on baseline [<sup>18</sup>F]FDG PET/CT, SUV<sub>max</sub> was analyzed on the follow-up scan after two cycles of [<sup>177</sup>Lu]Lu-PSMA-617 RLT. Response to the two cycles of [<sup>177</sup>Lu]Lu-PSMA-617 RLT was classified based on the change in lesional SUV<sub>max</sub> (i.e., radiotracer uptake) from the baseline [<sup>18</sup>F]FDG scan to the follow-up [<sup>18</sup>F]FDG scan. Positron Emission Tomography Response Criteria in Solid Tumors (PERCIST)<sup>37</sup> were used. According to these criteria, a ≥ 30% decrease from baseline SUV<sub>max</sub> was defined as a partial response, a < 30% decrease to a < 30% increase, as stable disease, and a ≥ 30% increase, as progression.

### Statistics

Descriptive statistics are reported as mean ± SD, median (minimum–maximum), and/or number (percentage) or vice versa, as applicable. The Mann–Whitney–U test was used to compare baseline SUV<sub>max</sub> of each radiotracer and baseline FPQ between the subgroup of lesions progressing after RLT versus the subgroup of non-progressing lesions, i.e. those exhibiting stable disease or partial response. Statistical significance was set at  $p < 0.05$ . All statistical analyses were carried out using Prism version 8 (GraphPad Software, San Diego, CA, USA). Variables showing a significant difference between lesion response subgroups were used to develop a lesion response prediction score for clinical application. For this score, points were assigned for different values of the respective variables with the goal of achieving a stepwise increment in lesional progression risk as the score increased.

Receiver operator characteristic (ROC) curve analysis was carried out to assess predictive performance of the significant variables and of the score. The performance metric was the area under the ROC curve (AUC). For each variable and for the predictive score, the maximum value of the Youden's index ( $J$ ) was used to determine the cut-off that attained optimal sensitivity and specificity.

### Ethics approval and consent to participate

All procedures performed in the patients described herein were in accordance with the ethical standards of the Institutional and/or National Research Ethics Committees and with the 1964 Helsinki Declaration and its later amendments, or with comparable ethical standards. This analysis was approved by the Institutional Review Board of the Ärztekammer des Saarlandes/Saarbrücken (approval number: 140/17, approval date: 13 July 2017). This report does not include any animal studies. Written informed consent was obtained from all participants.

### Results

Lesional values were highly variable for [<sup>68</sup>Ga]Ga-PSMA-11 SUV<sub>max</sub>, [<sup>18</sup>F]FDG SUV<sub>max</sub>, and FPQ, as reflected by large SDs relative to mean values and by wide minimum–maximum ranges (Table 2, Figs. 2 and 3). At baseline, 72/267 lesions (27.0%) had greater [<sup>18</sup>F]FDG uptake than [<sup>68</sup>Ga]Ga-PSMA-11 uptake i.e. an FPQ > 1, and 195/267 lesions (73.0%), equal or lesser [<sup>18</sup>F]FDG uptake than [<sup>68</sup>Ga]Ga-PSMA-11 uptake, i.e. an FPQ ≤ 1. Representative images of lesions showing different patterns of [<sup>18</sup>F]FDG and [<sup>68</sup>Ga]Ga-PSMA-11 uptake are seen in Fig. 4.

After two cycles of [<sup>177</sup>Lu]Lu-PSMA-617 RLT, relatively few lesions showed PERCIST progression pertaining to glucose metabolism: [<sup>18</sup>F]FDG SUV<sub>max</sub> increased ≥ 30% from baseline in 51/267 (19.1%) (Table 2). Of non-progressing lesions, a slight majority showed partial response (114/267, 42.7% of all analyzed lesions) versus stable disease (102/267, 38.2% of all analyzed lesions). Representative images of lesional responses are seen in Fig. 5.

At baseline, [<sup>68</sup>Ga]Ga-PSMA-11 SUV<sub>max</sub> was significantly lower in lesions that went on to progress after two RLT cycles than in lesions that went on to show stable disease or partial response ( $7.19 \pm 8.68$  vs.  $30.59 \pm 31.45$ ,  $p < 0.001$ ). Conversely, baseline [<sup>18</sup>F]FDG SUV<sub>max</sub> did not differ between these subgroups ( $8.79 \pm 5.47$  vs.  $10.22 \pm 7.11$ ,  $p = 0.29$ ) (Fig. 2A and B). However, the FPQ, i.e. the ratio of [<sup>18</sup>F]FDG uptake to [<sup>68</sup>Ga]Ga-PSMA-11 uptake, in progressing lesions significantly exceeded that in non-progressing lesions ( $2.65 \pm 3.16$  vs.  $0.60 \pm 0.63$ ,  $p < 0.001$ ) (Fig. 2C). Figure 3 depicts as waterfall plots the lesions' individual values for baseline [<sup>68</sup>Ga]Ga-PSMA-11 SUV<sub>max</sub> and baseline FPQ. No lesion with a baseline [<sup>68</sup>Ga]Ga-PSMA-11 SUV<sub>max</sub> ≥ 50 or a baseline FPQ < 0.5 showed [<sup>18</sup>F]FDG metabolic imaging progression.

On ROC curve analysis, baseline [<sup>68</sup>Ga]Ga-PSMA-11 SUV<sub>max</sub> and baseline FPQ showed similar performance to discriminate between lesions that would progress after two RLT cycles versus lesions that would not: respective AUCs were 0.89 versus 0.90. The respective maximum values of the Youden's index ( $J$ ) identified a baseline [<sup>68</sup>Ga]Ga-PSMA-11 SUV<sub>max</sub> of < 11.09 (Fig. 6A) or a baseline FPQ of ≥ 0.92 (Fig. 6B) as the threshold values of these variables that had optimal sensitivity and specificity in distinguishing lesional progression versus non-progression.

Characteristic/finding	Value		
Lesional $SUV_{max}$			
Baseline [ $^{68}\text{Ga}$ ]Ga-PSMA-11 PET/CT			
Median (minimum–maximum)	17.03 (0.35–185.83)		
Mean $\pm$ SD	26.12 $\pm$ 29.98		
Baseline [ $^{18}\text{F}$ ]FDG PET/CT			
Median (minimum–maximum)	7.94 (2.28–44.00)		
Mean $\pm$ SD	9.95 $\pm$ 6.84		
Baseline FPQ			
Median (minimum–maximum)	0.51 (0.03–15.54)		
Mean $\pm$ SD	0.99 $\pm$ 1.69		
Category, % of study sample (n)			
$\leq 1$	73.0% (195/267)		
$> 1$	27.0% (72/267)		
Lesional response <sup>a</sup> to RLT, % of study sample (n)			
Partial response	42.7% (114/267)		
Stable disease	38.2% (102/267)		
Progression	19.1% (51/267)		
	<b>Non-progressive lesions (n = 216)<sup>b</sup></b>	<b>Progressive lesions (n = 51)</b>	<b>p</b>
$SUV_{max}$ , baseline [ $^{68}\text{Ga}$ ]Ga-PSMA-11 PET/CT			
Median (minimum–maximum)	20.77 (1.03–185.80)	4.48 (0.35–48.25)	<b>&lt; 0.001</b>
Mean $\pm$ SD	30.59 $\pm$ 31.45	7.19 $\pm$ 8.68	
$SUV_{max}$ , baseline [ $^{18}\text{F}$ ]FDG PET/CT			
Median (minimum–maximum)	8.15 (2.28–44.00)	6.90 (3.69–27.37)	0.289
Mean $\pm$ SD	10.22 $\pm$ 7.11	8.79 $\pm$ 5.47	
FPQ, baseline PET/CT scans			
Median (minimum–maximum)	0.40 (0.03–3.81)	1.36 (0.51–15.54)	<b>&lt; 0.001</b>
Mean $\pm$ SD	0.60 $\pm$ 0.63	2.65 $\pm$ 3.16	

**Table 2.** PET variables of target lesions at baseline.  $^{18}\text{F}$  fluorine-18,  $^{68}\text{Ga}$  gallium-68, CT computed tomography, FDG fluorodeoxyglucose, FPQ [ $^{18}\text{F}$ ]FDG/[ $^{68}\text{Ga}$ ]Ga-PSMA-11  $SUV_{max}$  quotient, PET positron emission tomography, PSMA prostate-specific membrane antigen, RLT radioligand therapy, SD standard deviation,  $SUV_{max}$  maximum standardized uptake value. *p* values in bold were statistically significant at  $p < 0.05$ . <sup>a</sup>Lesional response classifications are based on change from baseline to post-2nd cycle of RLT in [ $^{18}\text{F}$ ]FDG  $SUV_{max}$ , utilizing PERCIST 1.0 criteria<sup>37</sup>. <sup>b</sup>“Non-progressing lesions” include those showing partial response (n = 114, 52.8% of non-progressing lesions) or stable disease (n = 102, 47.2% of non-progressing lesions).

At these thresholds, the two variables again showed comparable performance: respectively, 88.2% sensitivity and 81.9% specificity (OR 34.0), versus 90.2% sensitivity and 78.7% specificity (OR 34.0).

A clinical score incorporating the two variables, the dual imaging progression prediction (DIPP) score, was developed (Fig. 7A). Using ROC curve analysis, the DIPP score achieved an AUC of 0.94 to predict lesional response (Fig. 7B). The maximum value of the Youden's index (*J*) determined a DIPP score  $\geq 6$  on the 0–9-point scale to be the optimal threshold denoting high risk of lesional progression. With 88.2% sensitivity and 87.5% specificity (OR 52.5), this DIPP score threshold appeared to have comparable sensitivity, but appreciably improved specificity, relative to each of its component variables at their optimal thresholds.

## Discussion

This study is, to our knowledge, the first yet published that addresses the unmet need for lesion-based quantification of mismatch, by analyzing the relationship of baseline [ $^{68}\text{Ga}$ ]Ga-PSMA-11 and baseline [ $^{18}\text{F}$ ]FDG PET variables to RLT response, and introducing a scoring system that appears to effectively predict early lesional progression.

Our key finding was that efficient prediction of lesional response to RLT may be provided by considering not just the “traditional” eligibility criterion of PSMA ligand uptake, i.e.  $SUV_{max}$ , but an additional PET variable, the FPQ, i.e. the ratio of [ $^{18}\text{F}$ ]FDG  $SUV_{max}$  to [ $^{68}\text{Ga}$ ]Ga-PSMA-11  $SUV_{max}$ . Even better prediction may be achieved by using the DIPP score introduced here, which combines these two variables, and which can be easily and quickly calculated.

Our observation that the relationship of [ $^{18}\text{F}$ ]FDG  $SUV_{max}$  to [ $^{68}\text{Ga}$ ]Ga-PSMA-11  $SUV_{max}$  i.e. the FPQ, predicted lesional response to PSMA-targeted RLT, aligns with the findings of a number of studies suggesting predictive and prognostic power in prostate cancer of the [ $^{18}\text{F}$ ]FDG  $SUV_{max}$  of a lesion or of the total tumor burden. These studies showed these variables to be associated with negative disease characteristics and poor patient outcomes<sup>19–21,38–40</sup>, including in men with mCRPC<sup>18,22,41,42</sup>, and those undergoing PSMA-targeted RLT<sup>25,29</sup>.

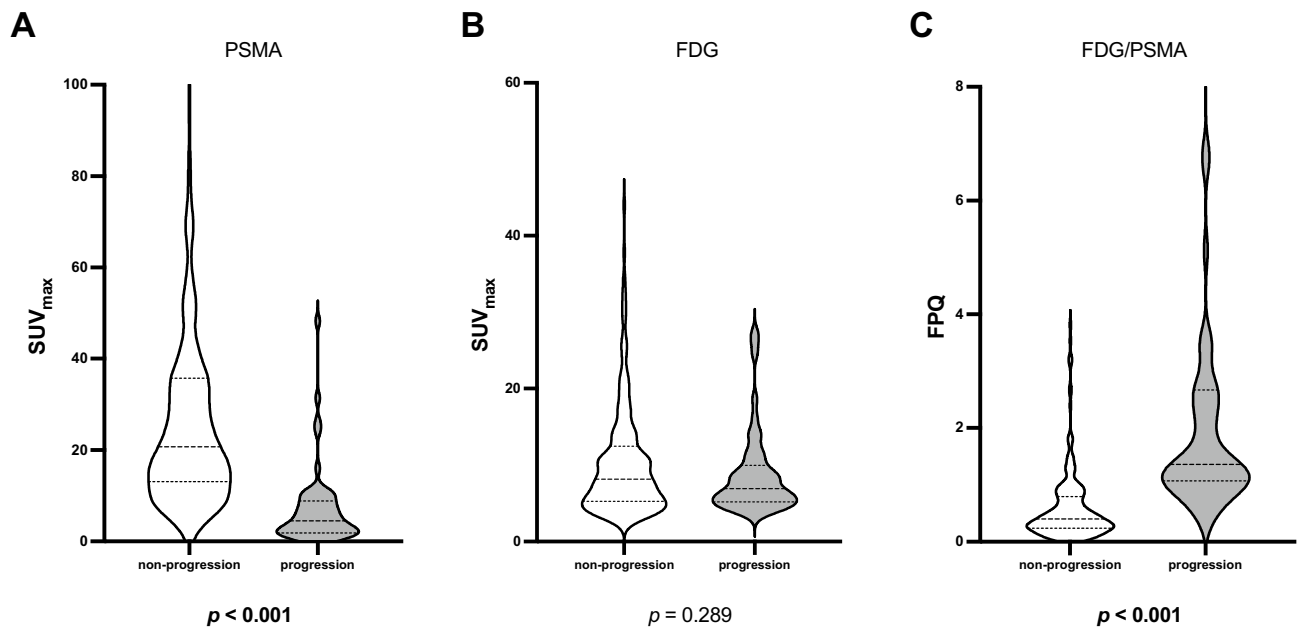


**Figure 2.** Baseline PET variables by lesional response to 2 cycles of [ $^{177}\text{Lu}$ ]Lu-PSMA-617 RLT: (A)  $\text{SUV}_{\text{max}}$  on [ $^{68}\text{Ga}$ ]Ga-PSMA-11 PET/CT, (B)  $\text{SUV}_{\text{max}}$  on [ $^{18}\text{F}$ ]FDG PET/CT, and (C) FPQ, [ $^{18}\text{F}$ ]FDG  $\text{SUV}_{\text{max}}$ /[ $^{68}\text{Ga}$ ]Ga-PSMA-11  $\text{SUV}_{\text{max}}$  quotient.

Thus, our analysis furnishes additional evidence buttressing use of [ $^{18}\text{F}$ ]FDG PET/CT in screening candidates for PSMA-targeted RLT.

However, our study also supplies evidence supporting the (unsurprising) primacy of PSMA ligand uptake in predicting lesional response to PSMA-targeted RLT. We noted that baseline [ $^{18}\text{F}$ ]FDG  $\text{SUV}_{\text{max}}$  alone did not differ between progressing and non-progressing lesions. By contrast, baseline [ $^{68}\text{Ga}$ ]Ga-PSMA-11  $\text{SUV}_{\text{max}}$  was a strong predictor of lesional progression to PSMA-targeted RLT both by itself (at a cut-off of  $< 11.09$ , 88.2% sensitivity and 81.9% specificity) and as part of the FPQ (at a cut-off of  $\geq 0.92$ , 90.2% sensitivity and 78.7% specificity). Moreover, considering PSMA ligand uptake as an absolute value as well as a relative value (i.e. as the denominator of the FPQ), combined into the DIPP score, further strengthened predictive performance (at a cut-off of  $\geq 6/9$  points, 88.2% sensitivity and 87.5% specificity).

Also of interest, there was an 80% rate of lesional stable disease or partial response in our study, notwithstanding the high degree of glucometabolism in many of the analyzed lesions. These observations support the notion that RLT may be beneficial even in lesions with high [ $^{18}\text{F}$ ]FDG uptake, so long as a sufficient proportion of cells has adequate PSMA expression—a factor that may be readily discerned using the FPQ. The benefit of RLT in such cases also has been suggested by others<sup>29,43</sup>.

A routine implementation of [ $^{18}\text{F}$ ]FDG PET/CT in clinical practice to screen candidates for PSMA-targeted RLT certainly brings additional information compared with a (contrast-enhanced) diagnostic CT but may have to be weighed against the potential financial burden regarding additional costs.

Based on our data, a mismatch lesion with insufficient PSMA expression and potential resistance to PSMA-targeted RLT can be identified by using the variables PSMA PET-derived  $\text{SUV}_{\text{max}}$  and FPQ. Compared to [ $^{68}\text{Ga}$ ]Ga-PSMA-11  $\text{SUV}_{\text{max}}$  or FPQ alone, a score combining both further strengthens predictive performance. We propose that a mismatch finding can be identified with a DIPP score of  $\geq 6$ . Quantitatively identifying mismatch lesions may facilitate individualized decision-making regarding PSMA-targeted RLT and the design of individualized mCRPC management strategies. However, the feasibility of implementing the DIPP score into clinical routine needs to be evaluated. We recommend studies, ideally prospective, in larger patient cohorts verifying our observations and addressing the clinical impact of this approach.

This analysis has several limitations. Firstly, the retrospective, single-center study design may impose bias and decrease generalizability and transferability. Other cutoff values would be expected for the use of different PSMA ligands or other reconstruction settings. Secondly, a possible selection bias cannot be excluded, as only a (pre-)selected number of patients who participated in the REALITY study received baseline and follow-up [ $^{18}\text{F}$ ]FDG PET/CT. The results of the present study should be treated with caution when compared with outcome data from other studies as our criterion of lesional progression was based on [ $^{18}\text{F}$ ]FDG PET/CT which is not established for prostate cancer such as response based on PSMA PET/CT or structural changes as reflected by Response Criteria in Solid Tumors<sup>44</sup>. Furthermore, our definition of progression was formulated on a lesional basis, not a patient basis. Further studies should be undertaken to consider relationships of PSMA ligand uptake and [ $^{18}\text{F}$ ]FDG uptake across the total tumor burden, e.g. in form of whole-body PET variables such as total lesion PSMA and total lesion glycolysis. These variables should be analyzed for their association with patient-based RLT response or overall survival. Lastly, we did not validate the DIPP score in a sample of lesions separate from those used to develop the score. The score's predictive performance should be confirmed in this way.

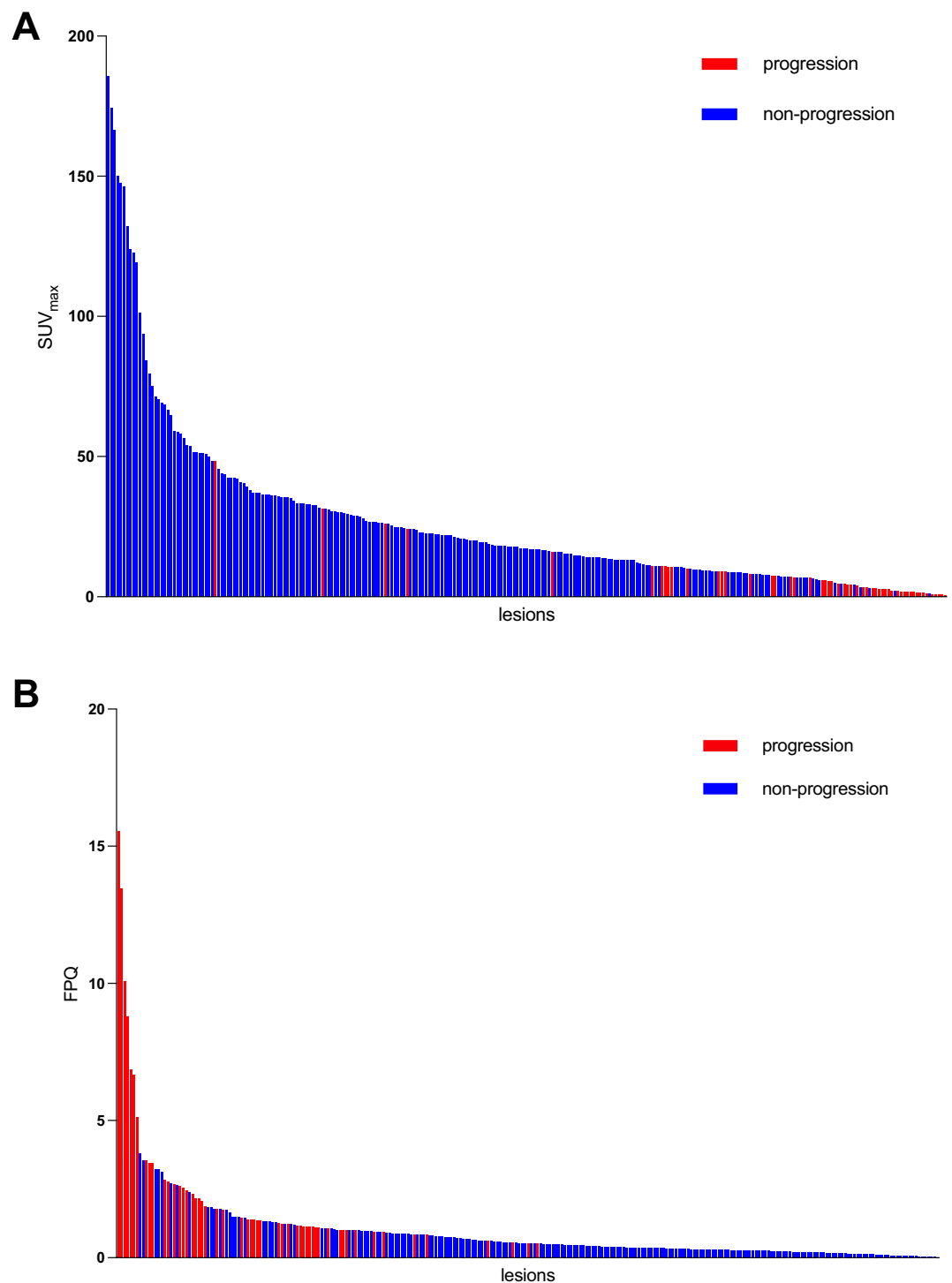


**Figure 3.** Waterfall plots showing lesional response to 2 cycles of [<sup>177</sup>Lu]Lu-PSMA-617 RLT by value of the lesional (A) SUV<sub>max</sub> on the baseline [<sup>68</sup>Ga]Ga-PSMA-11 PET/CT and (B) FPQ, [<sup>18</sup>F]FDG SUV<sub>max</sub>/[<sup>68</sup>Ga]Ga-PSMA-11 SUV<sub>max</sub> quotient.

### Conclusions

A low baseline SUV<sub>max</sub> on [<sup>68</sup>Ga]Ga-PSMA-11 PET/CT and high baseline FPQ, which incorporates the former as well as baseline [<sup>18</sup>F]FDG SUV<sub>max</sub>, predict lesional progression early in the course of RLT, whereas baseline [<sup>18</sup>F]FDG SUV<sub>max</sub> by itself does not. Compared to [<sup>68</sup>Ga]Ga-PSMA-11 SUV<sub>max</sub> or FPQ alone, a score combining

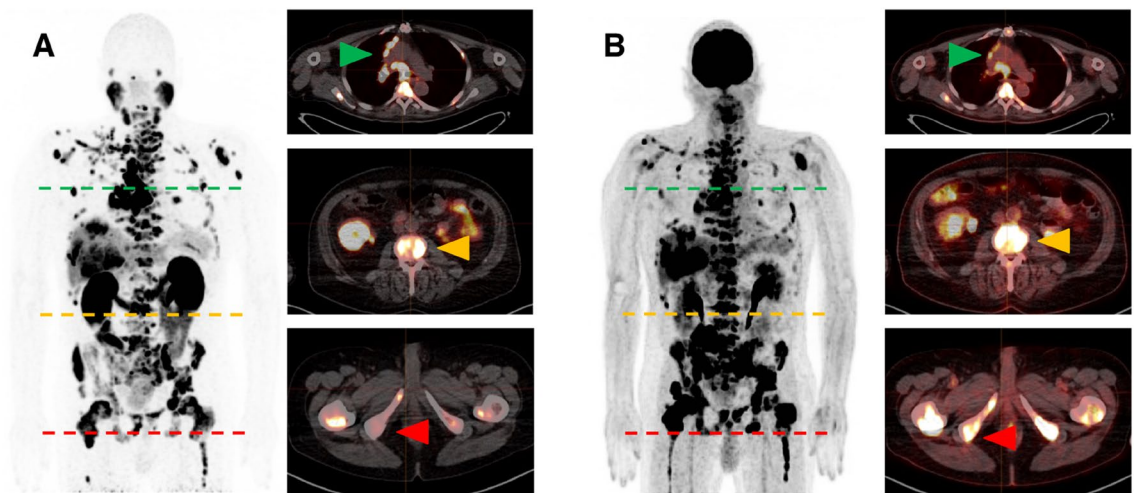


**Figure 4.** Representative whole-body and transversal slice images from (A) baseline  $[^{68}\text{Ga}]\text{Ga-PSMA-11}$  PET/CT scan and (B) baseline  $[^{18}\text{F}]\text{FDG}$ -PET/CT scan of a mCRPC patient showing different patterns of  $[^{68}\text{Ga}]\text{Ga-PSMA-11}$  uptake and  $[^{18}\text{F}]\text{FDG}$  uptake in different lesions. Green arrows denote lymph node metastases with intense  $[^{68}\text{Ga}]\text{Ga-PSMA-11}$  and moderate  $[^{18}\text{F}]\text{FDG}$  uptake. Yellow arrows indicate bone metastases with intense uptake of both radiotracers. Red arrows indicate bone metastases with faint  $[^{68}\text{Ga}]\text{Ga-PSMA-11}$  uptake but intense  $[^{18}\text{F}]\text{FDG}$  uptake.

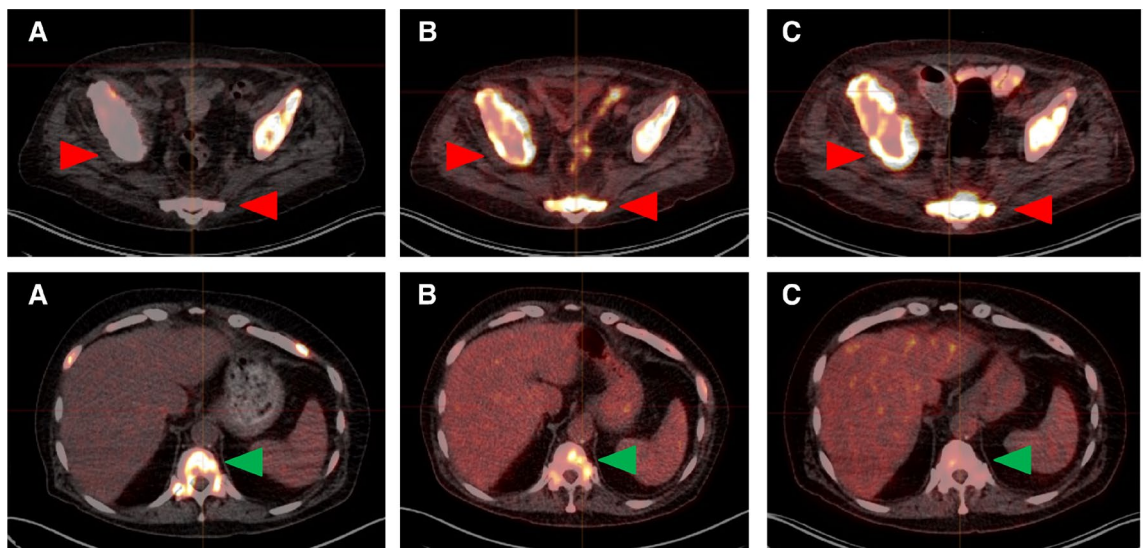


**Figure 5.** Representative transverse slice images showing lesion-based progression (first row) and partial response (second row) to 2 cycles of  $[^{177}\text{Lu}]\text{Lu-PSMA-617}$  RLT: (A) baseline  $[^{68}\text{Ga}]\text{Ga-PSMA-11}$  PET/CT, (B) baseline  $[^{18}\text{F}]\text{FDG}$  PET/CT, and (C) follow-up  $[^{18}\text{F}]\text{FDG}$  PET/CT. First row, red arrows: progressing bone metastases. These lesions had faint  $[^{68}\text{Ga}]\text{Ga-PSMA-11}$  uptake ( $\text{SUV}_{\text{max}}$ : 3.47 and 4.00, respectively) and intense  $[^{18}\text{F}]\text{FDG}$  uptake ( $\text{SUV}_{\text{max}}$ : 11.17 and 8.67, respectively) in the baseline scans (FPQ: 3.22 and 2.17, respectively), and increased  $[^{18}\text{F}]\text{FDG}$  uptake ( $\text{SUV}_{\text{max}}$  16.87 and 12.37, respectively; 51% higher and 43% higher, respectively, than at baseline) in the follow-up scan. Second row, green arrows: bone metastasis showing partial response. The lesion, which had intense  $[^{68}\text{Ga}]\text{Ga-PSMA-11}$  uptake ( $\text{SUV}_{\text{max}}$ : 22.74) and moderate  $[^{18}\text{F}]\text{FDG}$  uptake ( $\text{SUV}_{\text{max}}$ : 6.60) in the respective baseline scans (FPQ: 0.29), had decreased  $[^{18}\text{F}]\text{FDG}$  uptake ( $\text{SUV}_{\text{max}}$  4.52, 32% lower than at baseline) in the follow-up scan.

both predicts early lesional progression even more effectively and might therefore be useful to quantitatively identify mismatch lesions.



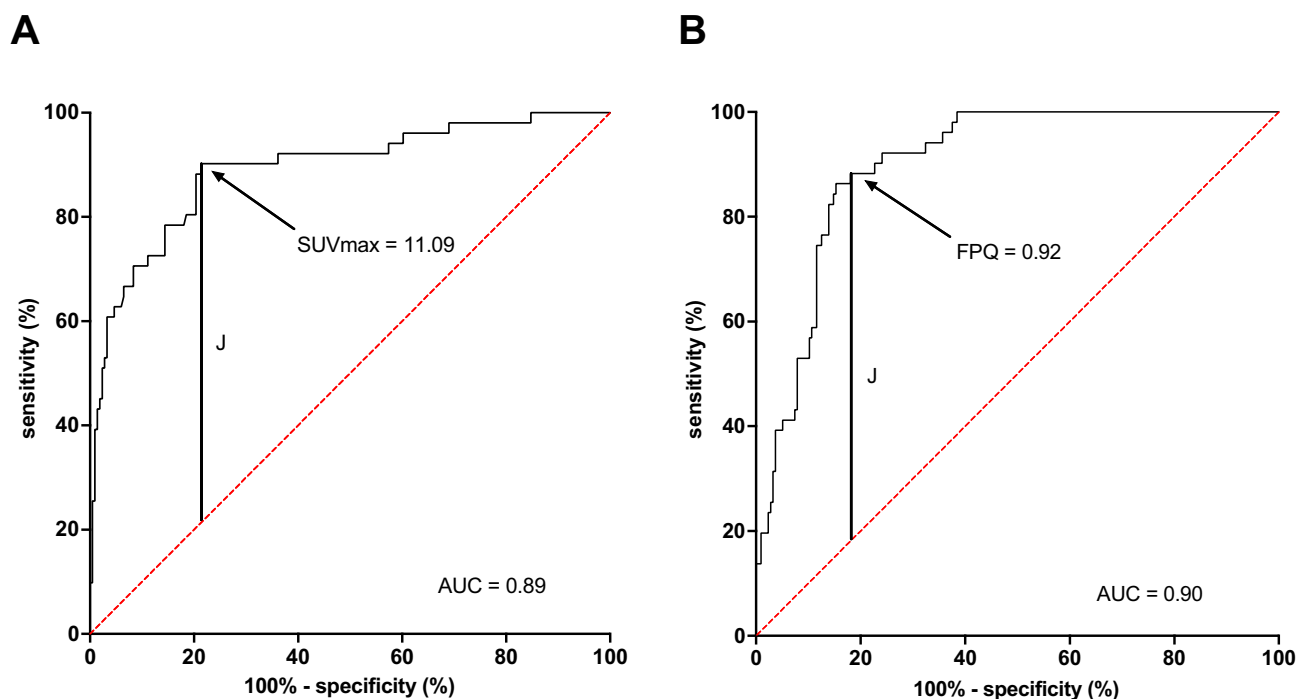


**Figure 6.** ROC curves showing the performance to predict lesional progression of (A) lesional  $SUV_{max}$  on the baseline  $[^{68}\text{Ga}]\text{Ga-PSMA-11}$  PET/CT scan or (B) FPQ,  $[^{18}\text{F}]\text{FDG } SUV_{max} / [^{68}\text{Ga}]\text{Ga-PSMA-11 } SUV_{max}$  quotient. The respective maximum values ( $J$ ) of the Youden's index identified a  $[^{68}\text{Ga}]\text{Ga-PSMA-11 } SUV_{max}$  of  $< 11.09$  (sensitivity 88.2%, specificity 81.9%) or an FPQ of  $\geq 0.92$  (sensitivity 90.2%, specificity 78.7%) as optimal thresholds.

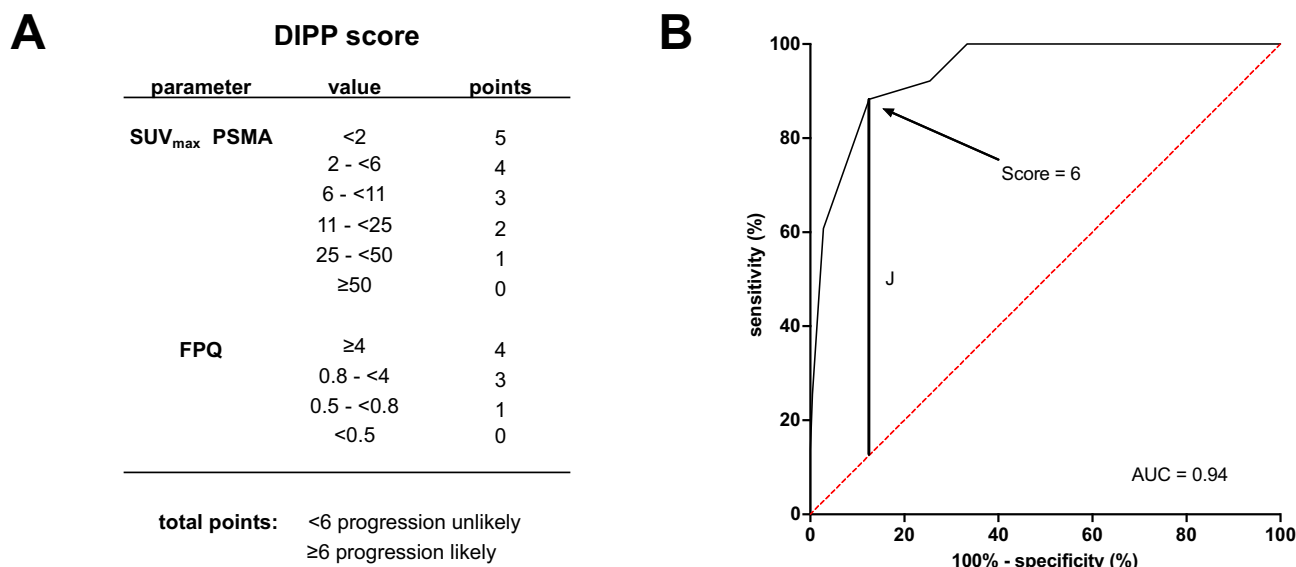


**Figure 7.** (A) Dual imaging progression prediction (DIPP) score and (B) ROC curve showing the score's performance to predict lesional progression. The maximum value of the Youden's index ( $J$ ) identified a DIPP score of  $\geq 6$  on a 0–9-point scale (sensitivity 88.2%, specificity 87.5%) as showing optimal predictive performance among DIPP score values.

### Data availability

The datasets used and analyzed during the current study are available from the corresponding author on reasonable request.

Received: 27 November 2023; Accepted: 13 May 2024

Published online: 17 May 2024

## References

- Sartor, O. *et al.* Lutetium-177-PSMA-617 for metastatic castration-resistant prostate cancer. *N. Engl. J. Med.* **385**, 1091–1103. <https://doi.org/10.1056/NEJMoa2107322> (2021).
- Hofman, M. S. *et al.* [(177)Lu]Lu-PSMA-617 versus cabazitaxel in patients with metastatic castration-resistant prostate cancer (TheraP): A randomised, open-label, phase 2 trial. *Lancet* **397**, 797–804. [https://doi.org/10.1016/S0140-6736\(21\)00237-3](https://doi.org/10.1016/S0140-6736(21)00237-3) (2021).
- Khreish, F. *et al.* 177 Lu-PSMA-617 radioligand therapy of metastatic castration-resistant prostate cancer: Initial 254-patient results from a prospective registry (REALITY Study). *Eur. J. Nucl. Med. Mol. Imaging* **49**, 1075–1085. <https://doi.org/10.1007/s00259-021-05525-7> (2022).
- Hofman, M. S. *et al.* Prostate-specific membrane antigen PET-CT in patients with high-risk prostate cancer before curative-intent surgery or radiotherapy (proPSMA): A prospective, randomised, multicentre study. *Lancet* **395**, 1208–1216. [https://doi.org/10.1016/S0140-6736\(20\)30314-7](https://doi.org/10.1016/S0140-6736(20)30314-7) (2020).
- Pienta, K. J. *et al.* A Phase 2/3 prospective multicenter study of the diagnostic accuracy of prostate specific membrane antigen PET/CT with (18)F-DCFPyL in prostate cancer patients (OSPREY). *J. Urol.* <https://doi.org/10.1097/JU.0000000000001698> (2021).
- Morris, M. J. *et al.* Diagnostic performance of (18)F-DCFPyL-PET/CT in men with biochemically recurrent prostate cancer: Results from the CONDOR phase III, multicenter study. *Clin. Cancer Res.* <https://doi.org/10.1158/1078-0432.CCR-20-4573> (2021).
- Afshar-Oromieh, A. *et al.* Performance of [(68)Ga]Ga-PSMA-11 PET/CT in patients with recurrent prostate cancer after prostatectomy—a multi-centre evaluation of 2533 patients. *Eur. J. Nucl. Med. Mol. Imaging* **48**, 2925–2934. <https://doi.org/10.1007/s00259-021-05189-3> (2021).
- Giesel, F. L. *et al.* Biochemical recurrence of prostate cancer: Initial results with [(18)F]PSMA-1007 PET/CT. *J. Nucl. Med.* **59**, 632–635. <https://doi.org/10.2967/jnumed.117.196329> (2018).
- Hohberg, M. *et al.* Biodistribution and radiation dosimetry of [(18)F]-JK-PSMA-7 as a novel prostate-specific membrane antigen-specific ligand for PET/CT imaging of prostate cancer. *EJNMMI Res.* **9**, 66. <https://doi.org/10.1186/s13550-019-0540-7> (2019).
- Dietlein, F. *et al.* An (89)Zr-labeled PSMA tracer for PET/CT imaging of prostate cancer patients. *J. Nucl. Med.* **63**, 573–583. <https://doi.org/10.2967/jnumed.121.262290> (2022).
- Rosar, F. *et al.* Detection efficacy of [(89)Zr]Zr-PSMA-617 PET/CT in [(68)Ga]Ga-PSMA-11 PET/CT-negative biochemical recurrence of prostate cancer. *Eur. J. Nucl. Med. Mol. Imaging* <https://doi.org/10.1007/s00259-023-06241-0> (2023).
- Burgard, C. *et al.* Detection efficacy of (68)Ga-PSMA-11 PET/CT in biochemical recurrence of prostate cancer with very low PSA Levels: A 7-year, two-center “real-world” experience. *Cancers (Basel)* <https://doi.org/10.3390/cancers15051376> (2023).
- Wright, G. L. Jr., Haley, C., Beckett, M. L. & Schellhammer, P. F. Expression of prostate-specific membrane antigen in normal, benign, and malignant prostate tissues. *Urol. Oncol.* **1**, 18–28. [https://doi.org/10.1016/1078-1439\(95\)00002-y](https://doi.org/10.1016/1078-1439(95)00002-y) (1995).
- Silver, D. A., Pellicer, I., Fair, W. R., Heston, W. D. & Cordon-Cardo, C. Prostate-specific membrane antigen expression in normal and malignant human tissues. *Clin. Cancer Res.* **3**, 81–85 (1997).
- Sweat, S. D., Pacelli, A., Murphy, G. P. & Bostwick, D. G. Prostate-specific membrane antigen expression is greatest in prostate adenocarcinoma and lymph node metastases. *Urology* **52**, 637–640. [https://doi.org/10.1016/s0090-4295\(98\)00278-7](https://doi.org/10.1016/s0090-4295(98)00278-7) (1998).
- Kratochwil, C. *et al.* Joint EANM/SNMMI procedure guideline for the use of (177)Lu-labeled PSMA-targeted radioligand-therapy ((177)Lu-PSMA-RLT). *Eur. J. Nucl. Med. Mol. Imaging* <https://doi.org/10.1007/s00259-023-06255-8> (2023).
- Eidelman, E., Twum-Ampofo, J., Ansari, J. & Siddiqui, M. M. The metabolic phenotype of prostate cancer. *Front. Oncol.* **7**, 131. <https://doi.org/10.3389/fonc.2017.00131> (2017).
- Bauckneht, M. *et al.* The prognostic power of 18F-FDG PET/CT extends to estimating systemic treatment response duration in metastatic castration-resistant prostate cancer (mCRPC) patients. *Prostate Cancer Prostatic Dis.* **24**, 1198–1207. <https://doi.org/10.1038/s41391-021-00391-8> (2021).
- Meziou, S. *et al.* GLUT1 expression in high-risk prostate cancer: Correlation with (18)F-FDG-PET/CT and clinical outcome. *Prostate Cancer Prostatic Dis.* **23**, 441–448. <https://doi.org/10.1038/s41391-020-0202-x> (2020).
- Lavallee, E. *et al.* Increased prostate cancer glucose metabolism detected by (18)F-fluorodeoxyglucose positron emission tomography/computed tomography in localised Gleason 8–10 prostate cancers identifies very high-risk patients for early recurrence and resistance to castration. *Eur. Urol. Focus* **5**, 998–1006. <https://doi.org/10.1016/j.euf.2018.03.008> (2019).
- Beauregard, J. M. *et al.* FDG-PET/CT for pre-operative staging and prognostic stratification of patients with high-grade prostate cancer at biopsy. *Cancer Imaging* **15**, 2. <https://doi.org/10.1186/s40644-015-0038-0> (2015).
- Suman, S. *et al.* Therapeutic efficacy, prognostic variables and clinical outcome of (177)Lu-PSMA-617 PRLT in progressive mCRPC following multiple lines of treatment: Prognostic implications of high FDG uptake on dual tracer PET-CT vis-a-vis Gleason score in such cohort. *Br. J. Radiol.* **92**, 20190380. <https://doi.org/10.1259/bjr.20190380> (2019).
- Khreish, F. *et al.* Value of combined PET imaging with [(18)F]FDG and [(68)Ga]Ga-PSMA-11 in mCRPC patients with worsening disease during [(177)Lu]Lu-PSMA-617 RLT. *Cancers (Basel)* <https://doi.org/10.3390/cancers13164134> (2021).
- Michalski, K., Mix, M., Meyer, P. T. & Ruf, J. Determination of whole-body tumour burden on [(68)Ga]PSMA-11 PET/CT for response assessment of [(177)Lu]PSMA-617 radioligand therapy: A retrospective analysis of serum PSA level and imaging derived parameters before and after two cycles of therapy. *Nuklearmedizin* **58**, 443–450. <https://doi.org/10.1055/a-1035-9052> (2019).
- Pathmanandavel, S. *et al.* The prognostic value of posttreatment (68)Ga-PSMA-11 PET/CT and (18)F-FDG PET/CT in metastatic castration-resistant prostate cancer treated with (177)Lu-PSMA-617 and NOX66 in a Phase I/II Trial (LuPIN). *J. Nucl. Med.* **64**, 69–74. <https://doi.org/10.2967/jnumed.122.264104> (2023).
- Adnan, A. & Basu, S. Concept proposal for a six-tier integrated dual tracer PET-CT (68Ga-PSMA and FDG) image scoring system (“Pro-PET” score) and examining its potential implications in metastatic castration-resistant prostate carcinoma theranostics and prognosis. *Nucl. Med. Commun.* **42**, 566–574. <https://doi.org/10.1097/MNM.0000000000001371> (2021).
- Adnan, A. & Basu, S. Comparison of dual-tracer PET and CT features to conventional risk categories in assessing response to (177)Lu-PSMA-617 therapy for metastatic prostate adenocarcinoma with urinary bladder involvement. *J. Nucl. Med. Technol.* **48**, 148–153. <https://doi.org/10.2967/jnmt.119.235960> (2020).
- Alberts, I. *et al.* Combined [(68)Ga]Ga-PSMA-11 and low-dose 2-[(18)F]FDG PET/CT using a long-axial field of view scanner for patients referred for [(177)Lu]-PSMA-radioligand therapy. *Eur. J. Nucl. Med. Mol. Imaging* **50**, 951–956. <https://doi.org/10.1007/s00259-022-05961-z> (2023).
- Michalski, K. *et al.* Prognostic implications of dual tracer PET/CT: PSMA ligand and [(18)F]FDG PET/CT in patients undergoing [(177)Lu]PSMA radioligand therapy. *Eur. J. Nucl. Med. Mol. Imaging* **48**, 2024–2030. <https://doi.org/10.1007/s00259-020-05160-8> (2021).
- Rosar, F. *et al.* Neuron-specific enolase has potential value as a biomarker for [(18)F]FDG/[(68)Ga]Ga-PSMA-11 PET mismatch findings in advanced mCRPC patients. *EJNMMI Res.* **10**, 52. <https://doi.org/10.1186/s13550-020-00640-2> (2020).
- Hofman, M. S. *et al.* [(177)Lu]-PSMA-617 radionuclide treatment in patients with metastatic castration-resistant prostate cancer (LuPSMA trial): A single-centre, single-arm, phase 2 study. *Lancet Oncol.* **19**, 825–833. [https://doi.org/10.1016/S1470-2045\(18\)30198-0](https://doi.org/10.1016/S1470-2045(18)30198-0) (2018).
- Hotta, M., Gafita, A., Czernin, J. & Calais, J. Outcome of patients with PSMA PET/CT screen failure by VISION criteria and treated with (177)Lu-PSMA therapy: A multicenter retrospective analysis. *J. Nucl. Med.* **63**, 1484–1488. <https://doi.org/10.2967/jnumed.121.263441> (2022).

33. Groener, D. *et al.* Baseline [(68)Ga]Ga-PSMA-11 PET/CT before [(177)Lu]Lu-PSMA-617 radioligand therapy: Value of PSMA-uptake thresholds in predicting targetable lesions. *Cancers (Basel)* <https://doi.org/10.3390/cancers15020473> (2023).
34. Jadvar, H. The VISION forward: Recognition and implication of PSMA-/(18)F-FDG+ mCRPC. *J. Nucl. Med.* **63**, 812–815. <https://doi.org/10.2967/jnumed.121.263274> (2022).
35. Fendler, W. P. *et al.* (68)Ga-PSMA PET/CT: Joint EANM and SNMMI procedure guideline for prostate cancer imaging: Version 1.0. *Eur. J. Nucl. Med. Mol. Imaging* **44**, 1014–1024. <https://doi.org/10.1007/s00259-017-3670-z> (2017).
36. Boellaard, R. *et al.* FDG PET/CT: EANM procedure guidelines for tumour imaging: Version 2.0. *Eur. J. Nucl. Med. Mol. Imaging* **42**, 328–354. <https://doi.org/10.1007/s00259-014-2961-x> (2015).
37. Wahl, R. L., Jacene, H., Kasamon, Y. & Lodge, M. A. From RECIST to PERCIST: Evolving considerations for PET response criteria in solid tumors. *J. Nucl. Med.* **50**(Suppl 1), 122S–S150. <https://doi.org/10.2967/jnumed.108.057307> (2009).
38. Meirelles, G. S. *et al.* Prognostic value of baseline [18F] fluorodeoxyglucose positron emission tomography and 99mTc-MDP bone scan in progressing metastatic prostate cancer. *Clin. Cancer Res.* **16**, 6093–6099. <https://doi.org/10.1158/1078-0432.CCR-10-1357> (2010).
39. Shen, K. *et al.* The evolving role of (18)F-FDG PET/CT in diagnosis and prognosis prediction in progressive prostate cancer. *Front. Oncol.* **11**, 683793. <https://doi.org/10.3389/fonc.2021.683793> (2021).
40. Oyama, N. *et al.* Prognostic value of 2-deoxy-2-[F-18]fluoro-D-glucose positron emission tomography imaging for patients with prostate cancer. *Mol. Imaging Biol.* **4**, 99–104. [https://doi.org/10.1016/s1095-0397\(01\)00065-6](https://doi.org/10.1016/s1095-0397(01)00065-6) (2002).
41. Fox, J. J. *et al.* Positron emission tomography/computed tomography-based assessments of androgen receptor expression and glycolytic activity as a prognostic biomarker for metastatic castration-resistant prostate cancer. *JAMA Oncol.* **4**, 217–224. <https://doi.org/10.1001/jamaoncol.2017.3588> (2018).
42. Jadvar, H., Desai, B. & Conti, P. S. Sodium 18F-fluoride PET/CT of bone, joint, and other disorders. *Semin. Nucl. Med.* **45**, 58–65. <https://doi.org/10.1053/j.semnuclmed.2014.07.008> (2015).
43. Current, K. *et al.* Investigating PSMA-targeted radioligand therapy efficacy as a function of cellular PSMA levels and intratumoral PSMA heterogeneity. *Clin. Cancer Res.* **26**, 2946–2955. <https://doi.org/10.1158/1078-0432.CCR-19-1485> (2020).
44. Eisenhauer, E. A. *et al.* New response evaluation criteria in solid tumours: Revised RECIST guideline (version 1.1). *Eur. J. Cancer* **45**, 228–47. <https://doi.org/10.1016/j.ejca.2008.10.026> (2009).

### Author contributions

Conceptualization, F.R., C.B., and S.E.; methodology, F.R. and C.B.; formal analysis, F.R., F.K. C.B. and S.D.; investigation, F.R., C.B., M.B., S.D., A.S.-S., S.M., S.P. and S.E.; data curation, F.R., C.B. and F.K.; writing—original draft preparation, F.R., C.B. and R.J.M.; writing—review and editing, all authors; visualization, F.R. and C.B.; supervision, S.E. All authors have read and agreed to the published version of the manuscript. All patients have given written consent to publication.

### Funding

Open Access funding enabled and organized by Projekt DEAL.

### Competing interests

The authors declare no competing interests.

### Additional information

**Correspondence** and requests for materials should be addressed to S.E.

**Reprints and permissions information** is available at [www.nature.com/reprints](http://www.nature.com/reprints).

**Publisher's note** Springer Nature remains neutral with regard to jurisdictional claims in published maps and institutional affiliations.



**Open Access** This article is licensed under a Creative Commons Attribution 4.0 International License, which permits use, sharing, adaptation, distribution and reproduction in any medium or format, as long as you give appropriate credit to the original author(s) and the source, provide a link to the Creative Commons licence, and indicate if changes were made. The images or other third party material in this article are included in the article's Creative Commons licence, unless indicated otherwise in a credit line to the material. If material is not included in the article's Creative Commons licence and your intended use is not permitted by statutory regulation or exceeds the permitted use, you will need to obtain permission directly from the copyright holder. To view a copy of this licence, visit <http://creativecommons.org/licenses/by/4.0/>.

© The Author(s) 2024